Author(s): Barikani, Mehdi; Saidpour, Hossein; Sezen, Mutlu
Article title: Mode-I Interlaminar Fracture Toughness in Unidirectional Carbon-fibre/Epoxy Composites
Year of publication: 2002
Citation: Barikani, M., Saidpour, H. and Sezen, M. (2002) 'Mode-I Interlaminar Fracture Toughness in Unidirectional Carbon-fibre/Epoxy Composites' *Iranian Polymer Journal*, 11 (6), pp. 413-423.
Published version available from: http://journal.ippi.ac.ir

Mode-I Interlaminar Fracture Toughness in Unidirectional Carbon-fibre/Epoxy Composites

Mehdi Barikani[1]*, Hossein Saidpour[2], and Mutlu Sezen[3]

(1) Department of Polyurethanes and Special Substances, Iran Polymer and Petrochemical Institute, P.O.Box: 4965/115, Tehran, I.R. Iran

(2) School of Engineering, University of East London, Dagenham, Essex, RMS 2AS, UK

(3) School of Design, Engineering & Computing, Bournemouth University, Dorset, BH12 5BB, UK

Received 6 April 2002; accepted 10 August 2002

ABSTRACT

High performance carbon fibre/epoxy composites, which are increasingly used for structural applications are susceptible to delamination. In response to this problem, the mode-I interlaminar fracture toughness of unidirectional carbon/epoxy laminates has been studied under tensile loading by using a double cantilever beam (DCB) specimen. The fracture energy is deduced from the data according to the area and the compliance methods. The morphology was explained through thermal analysis using DMA and fractography from scanning electron microscopy (SEM). Results showed improvement in high temperature moulding compound (HTM) system with 180°C cure in terms of interlaminar fracture toughness. There is also an improvement in MTM and LTM systems. SEM micrographs revealed their excellent delamination resistance as good crack stoppers with the evidence of strong fibre/matrix interface. For MTM systems G_{Ic} values dropped after post curing. This reduction was significant for MTM49-3 but not so much in the case of MTM49-7 laminate. On the other hand, the GIc for LTM45-1 did not seem to be affected by post curing at elevated temperature.

Iranian Polymer Journal, 11 (6), 2002, 413-423

Key Words:
fracture toughness;
delamination;
carbon / epoxy composite;
double catilever beam;
unidirectional.

INTRODUCTION

It is documented that development of approaches to toughening epoxy resins without sacrificing modulus and lowering the glass transition temperature would lead to an expansion of their use in areas such as primary and secondary aircraft structures, satellites, radomes, space structures, moulding compounds, motor racing industries and electrical and electronic components [1-3]. These materials are sensitive to defects, e.g. micro cracks, voids and interlaminar separations usually known as delamina-

(*)To whom correspondence should be addressed.
E-mail: M.Barikani@ippi.ac.ir

tion or debond, under service loading conditions. The defects may be as a result of residual stresses due to the curing process, external impact damage, environmental degradation or the fabrication process [4-9].

In many composites, the strength reduction has been observed due to delamination between plies. Delamination induced failure is normally a result of a combination of compressive and bending stresses caused by the delamination plies as they buckle out of plane. The strength reduction in an impact damaged laminate is, however, larger than that caused by delamination of an equivalent size. Therefore, impact damage cannot be represented by delamination alone. Fibre breakage and matrix cracking do have an effect on the strength and a delamination growing out of its plane is not likely to occur unless a considerable fibre breakage occurs. Sometimes the delamination extends to the edge of the material and may grow out of plane without any fibre breakage [10-12].

Interlaminar fracture is one of the major problems for fibre composites. Its occurrence greatly reduces the stiffness of a structure, often leading to catastrophic failure during service [13-14]. Thus, the resistance to delamination (interlaminar fracture toughness) is an important composite property of great interest to structural designers.

Life expectancy for composite structure requires a comprehensive understanding of the material's response to the growth of interlaminar delamination.

During the last decade, many investigations and scientific literature have been involved with interlaminar failure toughness (IFT) characterization of composite materials [15-22]. Most high performance composites are designed to have superior in-plane strength and stiffness such high performance is maintained in cases where the composite has homogeneous and continuous geometry. On the other hand, interlaminar performance is characterized by pronounced weakness under both shear and tensile stresses. Such interlaminar stresses become significant and affect the overall performance where geometrical and material discontinuities exist.

Several methods have therefore been developed for the measurement of interlaminar fracture toughness under various loading modes. The Double Cantilever Beam (DCB) test [23] is one of the methods designed to measure the interlaminar fracture toughness under interlaminar tensile stress, commonly known as mode-I. The main purpose is to characterize and compare the fracture toughness of different composite systems that consist of unidirectional fibres. The tests measure the energy necessary to produce an interlaminar crack between two plies of a composite material.

Rybicki et.al [24] realized that the critical energy release rate was useful to characterize delamination behaviour. The concept was further explored by many investigators [25-27]. Most of them employed double cantilever beam (DCB) specimens to determine G_{Ic} .

Aliyu and Daniel [28] used DCB specimens to investigate the mode-I interlaminar toughness of unidirectional AS4/3501-6 carbon/epoxy up to a crack speed of 51 mm/s. They found that the toughness increased with crack speed.

Subsequently Yaniv and Daniel [29] used a height-tapered double cantilever beam to produce higher crack speeds up to 26 m/s and found that the toughness increased with crack speed up to 1 m/s and, beyond that, it decreased with increasing crack speed.

Lambros and Rosakis [30] performed low velocity transverse impact tests on a quasi-isotropic laminate of a brittle graphite/ epoxy composite material. The impact-induced delamination was studied using an optical method and high speed photography. They found that the delamination crack speed could reach 1500 m/s. However, no interlaminar toughness was determined. In a sequel paper, they [31] produced high speed crack propagation in a unidirectional graphite/epoxy composite with a one-point bend set-up. Initiation fracture toughness was obtained. In order to relate the interlaminar toughness with crack propagation speed, Guo and Sun [32] used a conventional DCB specimen containing a tough adhesive film at the pre-crack tip to produce high speed mode-I crack propagation in polymeric composites. They found that the mode-I dynamic interlaminar fracture toughness of the unidirectional AS4/3501-6 was basically equal to the static fracture toughness for crack speeds under 200 m/s. However, the crack speeds produced in [32] are relatively low compared with the Rayleigh surface wave speed.

In this study an experimental work was carried out on unidirectional carbon/epoxy laminates. A double cantilever beam specimen was employed using corrected beam theory (CBT) method for calculating G_{Ic} (mode-I) in order to determine interlaminar fracture toughness evaluation of ACG40 series prepregs.

EXPERIMENTAL

Materials

Tests were carried out mainly on ACG40 series systems such as; HTM40, XHTM45, MTM49-7, MTM49-3 and LTM45-1 offering toughened laminates with impact resistance. The unidirectional reinforcements used were T800H, IM7 and AS4 carbon fibre with high strain to failure by different manufacturers. These carbon/epoxy prepregs were supplied by Advanced Composite Group (ACG) in UK.

Instrumental

An Acquati with 100 daN load cell tensile testing machine was used for IFT test and electron microscopy was conducted on a Philips 505 scanning electron microscope (SEM). Glass transition temperature was measured using Perkin Elmer dynamic mechanical analyzer (DMA).

Sample Preparation

All specimens consisted of 24 plies having 0°orientation, with the average of 60% fibre volume fraction. After the 12th ply, a 6 μm thick PTFE film was placed in the mid-plane to act as a crack starter. The film was 70 mm wide for G_{Ic} specimens. In order to ensure laminate quality, debulking was carried out at room temperature after every 4th ply. Following the lay up, laminates were vacuum bagged, sealed and cured using an autoclave as per the schedules shown in Table 1, followed by the free-standing post-cure in an air circulating oven.

Following the cure and post-cure procedure all the specimens were cut using a diamond circular saw with a nominal width (B) of 25mm and nominal length (L) of 125 mm for G_{Ic}. The edges were polished flat and smoothed. Two piano hinges were bonded onto the two sides of the specimen end with pre-crack. Hinges were glued to the specimens using 3M Scotch-weld and cured at 60 C for 15 min. Three identical specimens were produced for each specimen design.

Test Methodology

The G_{Ic} tests on ACG 40 series materials were performed according to ISO 95-12-12 and ASTM D5528-94a.

G_{Ic} Tests

The nominal thickness (2 h) was 3 mm as recommended for 60% VF CFRC. The double cantilever beam (DCB) specimens with piano hinges were placed in the Acquati tensile test machine using a 100-dan load-cell. Crack starter was 60μm thick PTFE film insert providing a nominal delamination length of a =50 mm from the load line. In order to monitor the crack propagation during loading, the edges of the specimens were marked up to 50 mm from the tip of the insert. The markings were made at 1 mm intervals for the first 10 mm, then at 5 mm intervals until 45 mm and again at 1 mm intervals for the last 5 mm (Figure 1).

Crack opening loads were applied through the piano hinges under displacement at 5 mm/min. The onset of delamination was monitored until the 5 mm-delamination length, then the specimen was unloaded. It was loaded again to monitor the mode-I pre-crack. Initiation of the crack and the propagation readings were recorded on the load-displacement curves. Data reduction yielded the critical energy release rates (G_{Ic}) for initiation and propagation of mode-I delamination. G_{Ic} was initially calculated by using the area method [33], which represents the area under the load-displacement curve. Area method is based on linear fracture mechanics simple beam theory, which assumes a perfectly built-in DCB specimen:

$$G_{Ic} = \frac{3P\delta}{2B\alpha}$$

where, P is the load (N), δ is the crack opening displacement (mm), B is the specimen width (mm), α is the delamination length (mm). However, this underestimates the compliance (C=δ/P) as the beam is not perfectly built-in. A means of correcting this effect is to apply a slightly longer delamination length of $\alpha + |\Delta|$. The $|\Delta|$ is found experimentally by plotting the cube

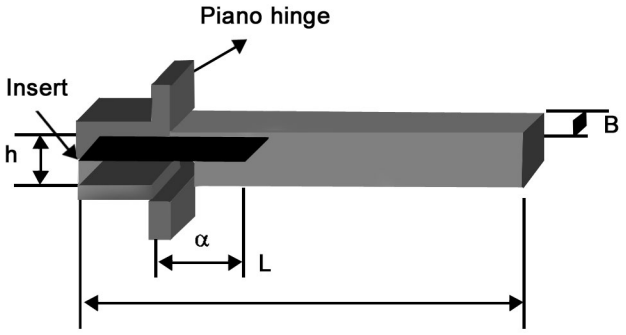

Figure 1. The schematic representation of the DCB specimen for mode-I (G_{Ic}) test.

root of compliance ($C_{1/3}$) against delamination length (α). The extrapolation of a linear fit through data yields Δ as the x-axis intercept.

The delamination propagation values from mode-I pre-crack were used for the linear fit data. In addition, large displacement correction (F) was applied for all specimens, which contributed significantly if the δ/p ratio was larger than 0.4. This method of calculating G_{Ic} is known as corrected beam theory (CBT). All initiation and propagation values were calculated according to:

$$GIc = \frac{3p\delta}{2B(a + |\Delta|} F$$

RESULTS AND DISCUSSION

The interlaminar fracture toughness was determined in terms of the mode-I critical strain energy release rate which may be regarded as G_{Ic}.There are three commonly used data reduction techniques; the compliance method, the direct method and the area method. The compliance methods used the load displacement plot to determine any non-ideal factors, the direct method requires knowledge of load displacement plot as well as material properties for such determination, and the area method employs changes in compliance to account for non-ideality. The values for IFT and T_g including the cure schedule and laminate details are given in Table 1.

G_{Ic} (Mode-I) Test Results

Mode-I pre-crack for starting the delamination yielded values higher than those obtained from the starter film (insert) values. All the quoted values summarized in Table 2 are based on mode-I fracture with a pre-crack that was initiated by the PTFE insert. For 40 series materials, XHTM45 system has the highest G_{Ic} critical

Table 1. ACG40 Series LTM/MTM/HTM composites, thermal and toughness related properties.

Prepreg systems	Cure schedule autoclave	Post cure (°c)	Tg (°c)	Mode-1 (G_{Ic}) J/m^2(area)	Mode-1 (G_{Ic}) J/m^2 (CBT)
HTM40/T800H	2 h at 180°C	None	188	430	332
XHTM45/IM7	2 h at 180°C	None	200	473	370
MTM49-7/T800H (MTM cure)	2 h at 135°C	None	152	290	230
		200	192	288	215
MTM49-7/T800H (LTM cure)	16 h at 80°C	None	130	235	170
		135	185	238	180
		200	206	239	158
MTM49-3/T800H (MTM Cure)	2 h at 135°C	None	168	230	200
		200	170	165	150
MTM49-3/T800H (LTM cure)	16 h at 80°C	None	106	300	235.5
		135	176	260	193.8
		200	179	205	147
LTM45-1\AS4	16 h at 60°C	None	--	--	144
		175	192	--	115

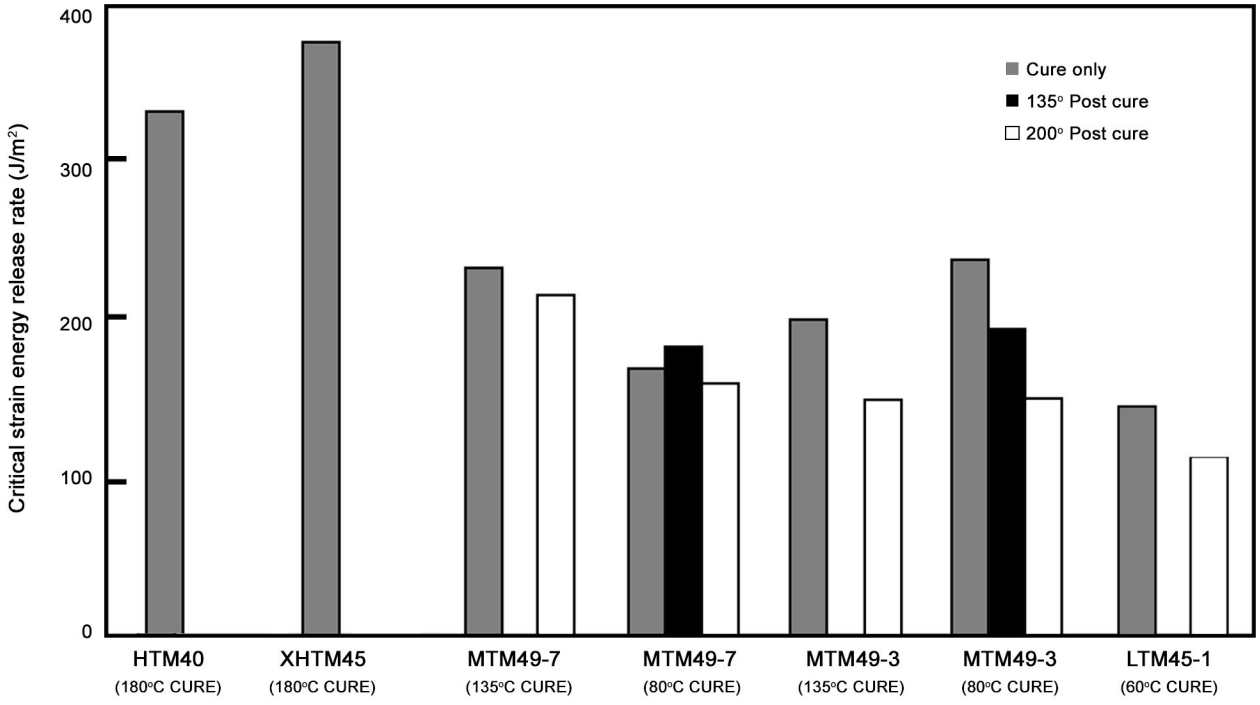

Figure 2. G_{Ic} critical strain energy release rates from mode-I pre-crack (calculated using Corrected Beam Theory).

strain energy release rate. The comparative values obtained from G_{Ic} tests are illustrated in Figure 2.

XHTM45 showed the highest G_{Ic} value amongst the materials tested. G_{Ic} value for HTM40 was lower than XHTM45 but higher than MTM49-7 and MTM49-3. R-curve showed that the crack resistance was established after the highest load, but G_{Ic} increased up to 450 J/m² beyond the 80 mm delamination length.

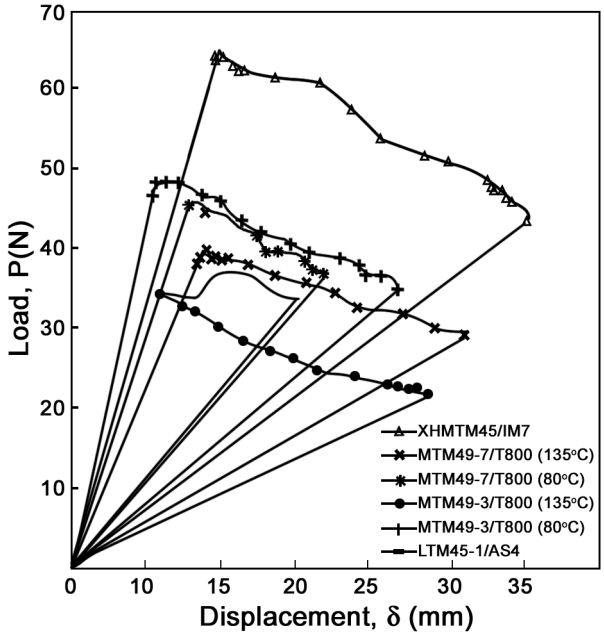

Figure 3. G_{Ic} (mode-I) load versus displacement representative curves for each material.

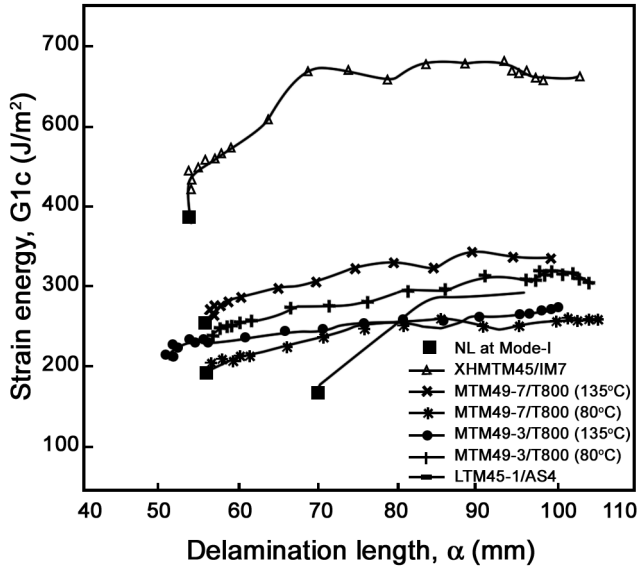

Figure 4. R-curves (resistance curves), G_{Ic} propagation values against delamination growth for mode-I loading.

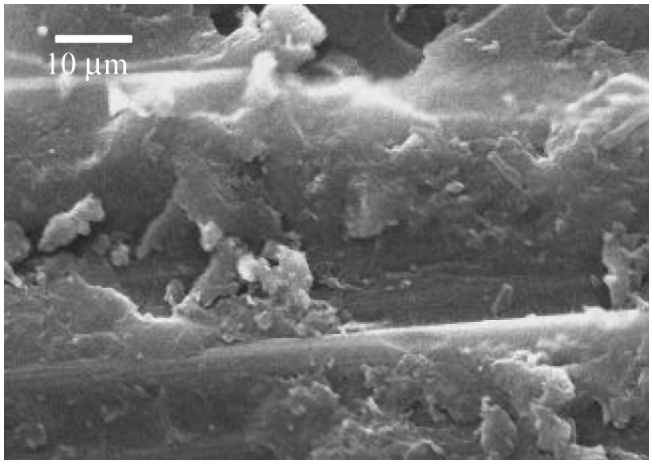

(a) HTM40/T800 180°C/2h (1000x).

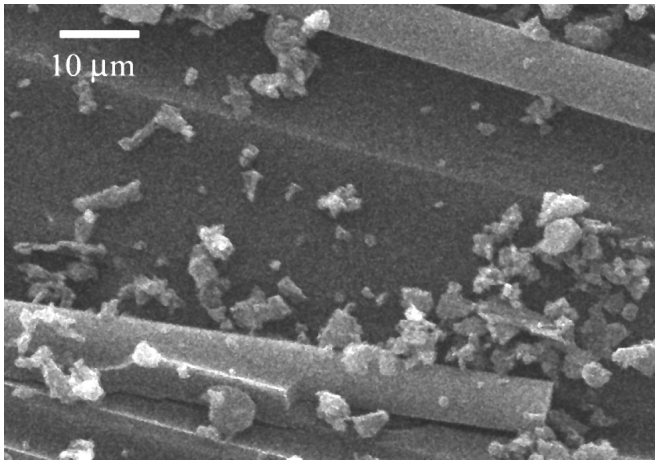

(c) LTM45-1/AS4 60°C/16h cure (1000x).

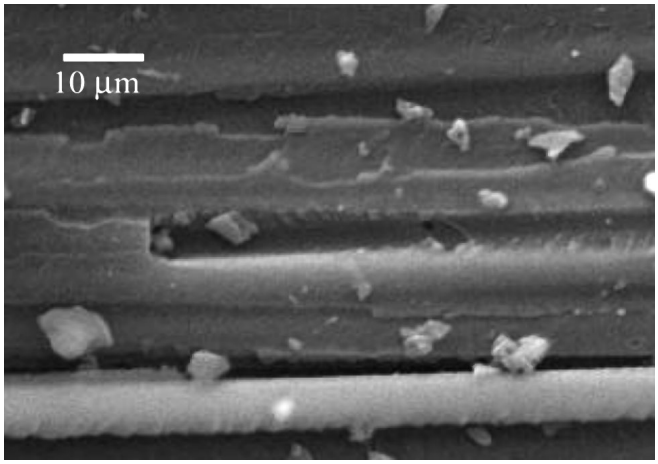

(b) XHTM45/IM7 180°C/2h (1000x).

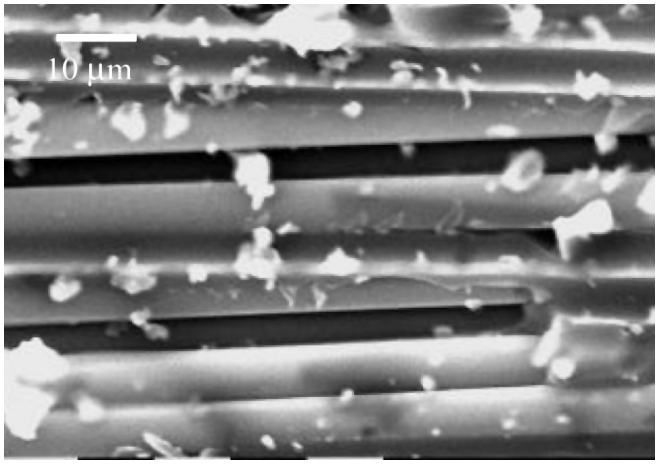

(d) LTM45-1/AS4 60°C/16h + 175°C post-cure (1000x).

Figure 5. SEM Micrographs showing fracture surfaces of mode-I failure for LTM and HTM systems.

HTM40 is however a tough system with good impact and delamination resistance.

When MTM49-7 cured at 135 C for 2 h, it showed adequate G_{lc} value but not as mush as HTM cure materials. After post cured at 200 C, G_{lc} dropped slightly. R-curves in Figure 4 showed that it had highest Glc after 200 C post-cure amongst the MTM49 materials tested.

For MTM49-3 and MTM49-7 systems, G_{Ic} values dropped after post-curing. This reduction was significant for MTM49-3 but not so much in the case of MTM49-7 laminate, although there is a slight improvement on G_{Ic} for MTM49-7 at 135 C post cure. On the other hand, the G_{Ic} for LTM45-1 also seems to be affected by post-curing at elevated temperature. LTM45-1 had the lowest G_{lc} value.

For the load versus displacement curves in Figure 3, the first marked point corresponds to the onset of delamination. Besides the initiation and the maximum point, propagation values were also marked for each delamination length during crack propagation from mode-I pre-crack. The reduction in the load level after the maximum level was more of the same for all materials showing a consistency on load reduction during delamination.

The lowest initiation and the following propagation values were used to draw the resistance curves (R-curves) against the delamination growth in Figure 4. After the maximum G_{Ic} obtained the crack growth showed an almost stable plateau that standard devia-

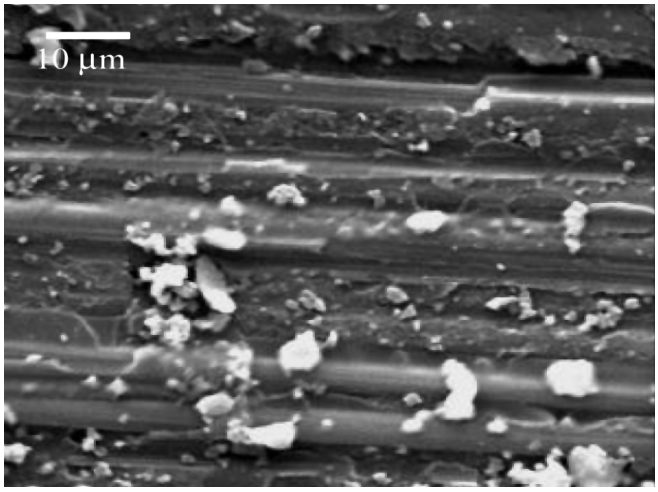

(a) MTM49-7/T800 135°C/2 h cure (1000x).

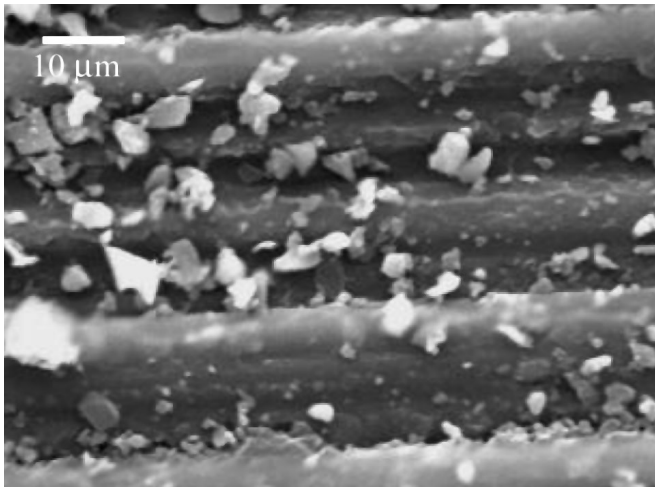

(c) MTM49-7/T800 80°C/16 h cure (1000x).

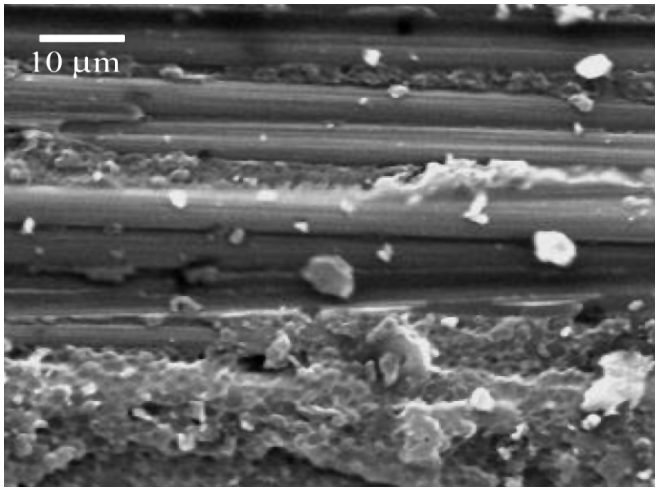

(b) MTM49-7/T800 135°C/2 h+200°C post-cure (1000x).

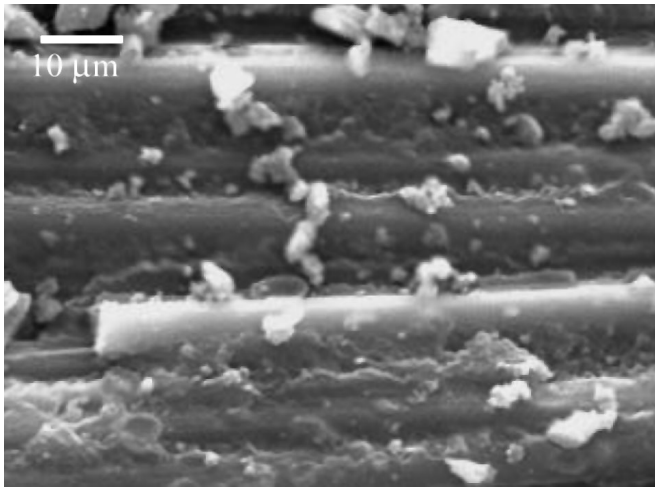

(d) MTM49-7/T800 80°C/16 h+135°C post-cure (1000x).

Figure 6. SEM Micrographs showing fracture surfaces of mode-I failure for MTM49-7/T800 system (10 µm).

tions of the propagation values did not exceed 10% of the average values.

Fractography (SEM)

Investigations of impact damage and fracture surfaces by SEM are necessary to determine the failure criteria and further to identify the mechanism involved in toughening by observing the phase morphology in cross-linked epoxy matrix structure. Furthermore, the neat resin fracture analysis should indicate the concentration and dispersion of the toughness. It should help to optimize level of toughness modification and hopefully relate to results obtained from composite fracture toughness tests.

All fractured surfaces were subsequently examined in a scanning electron microscopy to determine the degree of resin fracture. The nature of resin fracture (brittle versus ductile) and the degree of micro cracking which precedes the fracture were determined by hackles [34] on the fractured surfaces. Fracture surfaces of mode-I specimens are shown in Figures 5-7.

Brittle fracture from mode-I (G_{Ic}) failure was characterized by a smooth corrugated surface [35], which could also be the result of fibre debonding [36] in the interface. However, the weak interface does not necessarily refer to low fracture toughness. Interfacial failures somehow cause fibre bridging that enhances the delamination growth and combined with fibre pull-out will dissipate additional energy. Therefore, the critical strain energy will probably be less than the actual neat-

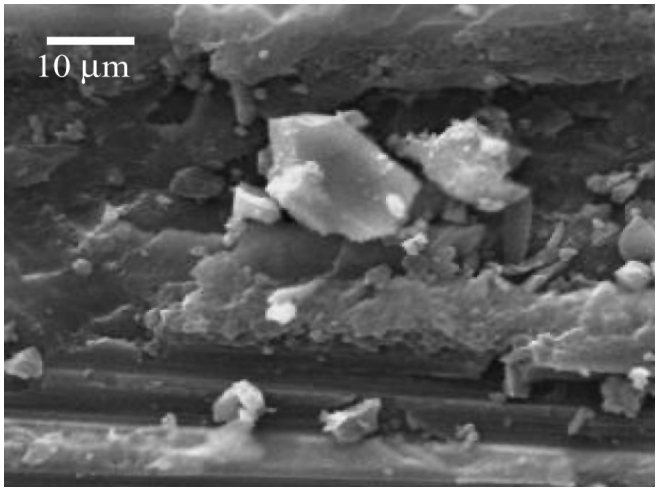

(a) MTM49-3/T800 135°C/ 2 h cure (1000x).

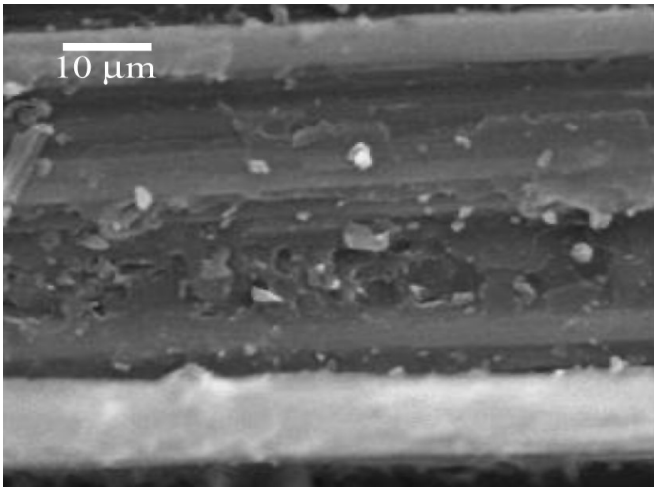

(c) MTM49-3/T800 80°C/16 h cure (1000x).

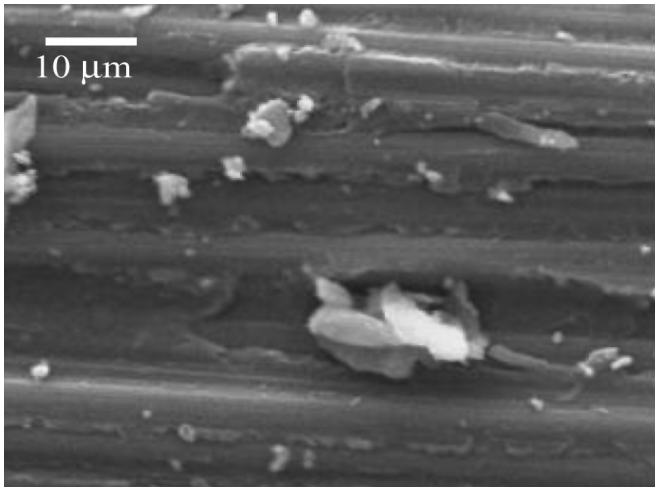

(b) MTM49-3/T800 135°C/ 2 h+200°C post-cure (1000x).

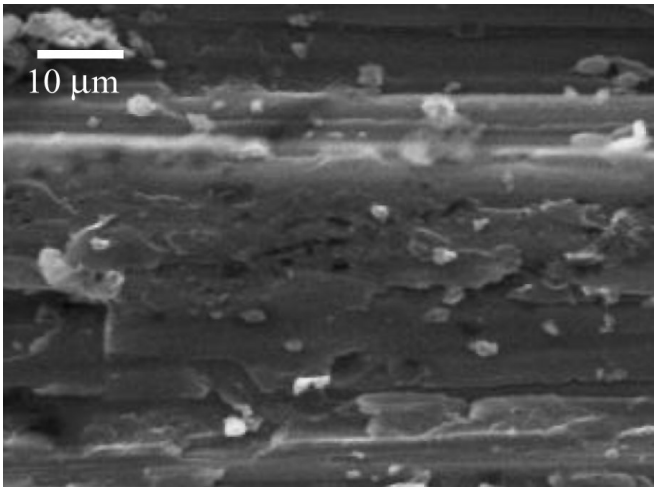

(d) MTM49-3/T800 80°C/16 h+135°C post-cure (1000x).

Figure 7. SEM Micrographs showing fracture surfaces of mode-I failure for MTM49-3/ T800 system.

resin fracture toughness because the interfacial failure inhibits the higher strain-to-failure. The existence of fibres in a laminate does constrain the plastic zone strongly and it affects the stress level at the critical strain at the crack tip. This will in turn prevent the efficient translation of the resin toughness into composite fracture toughness.

In the LTM systems after post cure, the mode-I delamination is dominated by interfacial debonding. XHTM45 showed the highest G_{Ic} value amongst the materials tested. R-curve showed increasing energy levels as the crack propagated at which the G_{Ic} reached about 500 J/m^2. Micrographs from G_{Ic} indicate strong interface, also evident was the hackle markings on the resin which did not come off the fibres as the delamination occurred.

Micrographs also revealed its excellent delamination resistance with elongated hackles. The transverse cracks in resin were perpendicular to fibre. A few resin fractures was at right angle to fibres then changing direction with resin elongation as the crack propagated. This is a very good way of absorbing energy under shear loading. Thus, XHTM45 type is a good crack stopper with high delamination resistance and strong fibre/matrix interface (Figure 5). As well as its improved toughness, XHTM45 showed high temperature performance capability with T_g reaching up to 200 C with increased modulus retention at high temperature.

HTM40 had a lower G_{Ic} value than XHTM45 type

but higher than MTM49-3 and -7. R-curve showed that the crack resistance was stabilized after the highest load, but G_{Ic} increased up to 450 J/m² beyond the 80 mm delamination length. SEM revealed a strong fibre/matrix adhesion with ductile failure as the fibres were still covered with resin after the failure (Figure 4). DMA indicated a fully cross-linked structure with T_g value of 188 C (Table 1).

When MTM49-7 cured at 135 C for 2 h, it showed adequate G_{Ic} value but not as much as HTM cure materials. After post-cured at 200 C, G_{Ic} dropped slightly. R-curves showed that it had the highest G_{Ic} after 200 C post-cure amongst the MTM49 materials tested (Figure 4). DMA tan δ traces showed that the modulus retention was also better after post-curing with T_g increasing up to 192 C (Table 1).

When systems cured at 80 C for 16 h, the G_{Ic} was much lower. The value improved very slightly after 135 C post-cure but further dropped after 200 C post-cure (Table 1). SEM showed G_{Ic} failure was resin dominant that fairly ductile resin failure without strong resistance to crack growth. As the material was post-cured, the interfacial debonding became more evident with signs of resin shrinkage as shown in micrographs (Figure 6).

After the initial cure of MTM49-3 at 135 C for 2 h, the G_{Ic} value was lower than the value for MTM49-7, but the reduction in G_{Ic} after the 200 C post-cure was much higher. Micrographs of the mode-I fracture showed strong fibre/resin bond for the material without post cure as more fibres were covered with resin and less resin fragments spread around (Figure 7). After 200 C post-cure, more resin fragments were observed and as the fibres failed they left imprints of on the resin. Thus the interfacial adhesion was lowered with post-cure, but the ability of the material to absorb fracture energy was increased.

As the T_g of the samples increased with post curing at 135 C and 200 C the tan δ peak is reaching single and sharper it shows that MTM49-3 system was not fully phase separated after curing 16 h at 80 C.
G_{Ic} was the highest after cure only and it was drapped as it was post cured. SEM micrographs show that the failure became more brittle as the interfacial strength was reduced (Figure 7).

For LTM45-1 system, the G_{Ic} test was performed according to ASTM and it was calculated from insert rather than mode-I pre-crack. It showed the lowest G_{Ic} value of 144 J/m², which was reduced to 115 J/m² after the post-cure at 175 C.

The SEM micrographs (Figure 5) show the severe fibre debonding that was evident after G_{Ic} failure. The brittle nature of the resin resulted in debonding as seen on the micrograph by the resin particles scattered around. This indicated the low interfacial toughness of the material due to crack growth under tensile loading. The energy absorption level after the initial crack was, however, increased as the delamination grew and reached a plateau of 275 J/m² level.

CONCLUSION

HTM systems with 180 C cure showed improved toughness in terms of fracture toughness property and high fracture toughness was obtained with 180 C cured HTM systems. SEM micrographs revealed their excellent delamination resistance as good crack stoppers together with the evidence of strong fibre/matrix interface.
G_{Ic} values of LTM cure materials were reduced with post cure due to the build up of the internal stresses during post cure. This was supported with appearance of interfacial debonding in the SEM microgrpahs. The resin shrinkage seems to play an important role in this reduction of the interfacial bond. This in turn reduced the ability of the material to sustain delamination growth under mode-I loading.

Dynamic mechanical analysis (DMA) indicated that increased T_g of the LTM and MTM prepregs after post-curing at elevated temperatures. The variations observed in the shift of tan δ peaks after each post cure. This could be related to increased toughness performance of the LTM materials. The failure mechanisms seem to be different for different tough matrix materials and appear to be strongly dependent on the cure and post curing conditions. This is particularly noticeable for curing at 135 C and 80 C.

ACKNOWLEDGEMENTS

The authors would like to thank Advanced Composites Group (U.K.) for funding this project and for providing the materials. Authors' appreciation is given to Mr Majid Barikani for his assistance in type setting the manuscript.

REFERENCES

1. Anderson G.J, Charles S.B., and Kropp M.A., Polyimide hybride adhesives , *US Patent* 6,294,259 (2001).
2. Barkoula N.M., Popanicolaou G.C., and Kargerkocsis J. Prediction of the residual tensile strengths of carbon fibre/ epoxy laminates with and without interleaves after solid particle erosion , *Comp .Sci. & Tech.,* **62**, 121-130 (2002).
3. Wu H., Gopala A., Harris F., and Heiden P., Investigation of readily processable thermoplastic toughened thermoplastic , *J. Appl. Polym.Sci.,* **70**, 5, 935-951 (1998).
4. Nageswara R.B. and Acharya A.R., Evaluation of fracture energy G_{Ic} using a double cantilever beam fibre composite specimen , *Eng. Frac. Mech.,* **51**, 2, 317-322 (1995).
5. Dransfield K.A., Jain L.K., and Mai Y.W., On the effects of stitching in CFRPs-I. Mode I delamination toughness , *Comp. Sci. & Tech.,* **58**, 813-827 (1998).
6. Choi H.Y. Downs R.J., and Chang F-K., A new approach towards understanding damage mechanisms and mechanics of laminated composites due to low velocity impact , *J. Comp. Mat.,* **25**, 992-1011 (1991).
7. Abrate S. Impact on laminated composites: Recent advances , Appl. Mech. Rev., **47**, 11, 517-544 (1994).
8. Compston P., Jar P.Y.B., and Davies P., Matrix effect on the static and dynamic interlaminar fracture toughness of glass-fibre marine composites , *Composites,* **29B**, 505-516 (1998).
9. Tsai J.L., GUO C. and Sun C.T., Dynamic delamination fracture toughness in unidirectional polymeric composites , *Comp. Sci. & Tech.,* **61**, 87-94 (2001).
10. Compston P., Jar P.Y.B., Burchill P.J., and Takahashi K. The effect of matrix toughness and loading rate on the mode II interlaminar fracture toughness of glass fibre/vinyl ester composites , *Comp. Sci. & Tech.,* **61**, 321-333, (2001).
11. Albertsen H., Ivens J., Peters P., Wevers M., and Verpoest I., Interlaminar fracture toughness of CFRP influenced by fibre surface treatment: part 1 experimental results , *Comp. Sci. & Tech.,* **54**, 133-145 (1995).
12. Benzeggagh M.L. and Benmedakhene S., Residual strength of glass/propylene composite material subjected to impact , *Comp. Sci. & Tech.,* **55**, 1-11 (1995).
13. Todo M., Jar P.Y.B, and Takahashi K., Initiation of a mode II interlaminar crack from an insert film in the end-notched flexure composite specimen , *Comp. Sci. & Tech.,* **60**, 263-272 (2000).
14. Sohn M.S. and HU X.Z., Comparative study of dynamic and static delamination behaviour of carbon fibre/epoxy composite laminates , *Composites,* **26**, 849-858 (1995).
15. Hunston D.L., Characterisation of interlaminar crack growth in composites with the double cantilever beam specimen , In: *Tough Composite Materials,* Proceeding of a workshop held at NASA Langley Research Centre, Hampton, Virginia, May 24-26, 3-17., NASA Conference publication No 2334 (1983).
16. Kageyama K. et al. Mode-I and mode-II delamination growth of interlayer toughened carbon/epoxy composite systems , In: *Composite Materials :Fatigue and Fracture*-5th vol. ASTM STP Martin R.H (Ed.) Philadelphia, 19-37 (1995).
17. Singh S. and Partridge I.K., Delamination failure in unidirectional carbon fibre/epoxy under mixed mode loading *Polym. & Polym. Comp.,* **3**, 1, 35-39 (1995).
18. Todo M. and Jar P.Y.B., Study of mode-I interlaminar crack growth in DCB specimens of fibre reinforced composites , *Comp. Sci. & Tech.,* **58**, 105-118 (1998).
19. ASP LE., The effects of moisture and temperature on the interlaminar delamination toughness of a carbon/epoxy composite , *Comp. Sci. & Tech.,* **58**, 967-977 (1998).
20. Hwang S.F. and Cherng Shen B., Opening-mode interlaminar fracture toughness of interply hybride composite materials , *Comp. Sci. & Tech.,* **59**, 1861-1869 (1999).
21. Tai N.H., Yip M.C., and Lin J.L., Effect of low energy impact on the fatigue behaviour of carbon/epoxy composites , *Comp. Sci. & Tech.,* **58**, 1-8 (1998).
22. Todo M. and Jar P.Y.B. Study of mode 1 interlaminar crack growth of fibre reinforced composites using DCB specimens , C*omp. Sci. & Tech.,* **58**, 105-118 (1998).
23. Wilkins D.J., Eisenmann J.R., Camin R.A., Margolis W.S., and Benson R.A., Characterization delamination growth in graphite/epoxy damage in composite materials , *ASTM STP 775,* 168-183 (1982).
24. Rybicki E.F. Schmueser D.W., and Fox T. J. An energy release rate approach for stable crack growth in the free-edge delamination problem *Comp. Mat.,* **11**, 470-487 (1977).
25. Davitt D.F., Schapery R.A., and Bradley W.L., A method for determining mode 1 delamination fracture toughness of elastic and viscoelastic composite materials , *J. Comp. Mat.,* **14**, 270-285 (1980).
26. Davies P., Moulin C., Kauch H.H., and Fisher M., Measurement of G_{Ic} and G11c in carbon/epoxy com , *Comp. Sci. & Tech.,* **39**, 193-205, 1990.

27. Caprino G., The use of thin DCB specimens for measuring mode 1 interlaminar fracture toughness of composite materials , *Comp. Sci. & Tech.*, **39**, 2, 147-158 (1990).
28. Aliyu AA. and Daniel IM., Effects of strain rate on delamination fracture toughness of graphite/epoxy . In: *Delamination and Debonding of Materials*, Johnson *ASTM STP* 876, Philadelphia, PA: American Society for Testing and Materials, 336-348 (1985).
29. Yaniv G. and Daniel I.M., Height-tapered double cantilever beam specimen for study of rate effects on fracture toughness of composites . In: *Composite Materials: Testing and Design*, Whitcomb J.D., Ed., (8th Conference), *ASTM STP* 972, Philadelphia ,PA: American Society for Testing and Materials, 241-258 (1988).
30. Lamboros J. and Rosakis A.J., Experimental investigation of dynamic delamination in thick polymeric composite laminates , *Exp. Mech.*, **37**, 3, 360-336 (1997).
31. Lamboros J. and Rosakis A.J., Dynamic crack initiation and growth in thick unidirectional graphite/epoxy plates , *Comp. Sci. & Tech.*, **57**, 55-65 (1997).
32. Guo C. and Sun C.T., Dynamic mode I crack propagation in carbon/epoxy composite , *Comp. Sci. & Tech.*, **58**, 1405-10 (1998).
33. Whitney J.M., Browning C.E., and Hoogsten W., A double cantilever beam test for characterising mode I delamination of composite materials , *J. Rein. Plas. & Comp*. **1**, 297-313 (1982).
34. Morris G.E., Determining fracture directions and fracture origins on failed graphite/epoxy surfaces. Non destructive evaluation and flaw criticality for composite materials , *ASTM STP* 696, Pipes R.B. (Ed.) 274-297 (1979).
35. Bradley W.L., Relationship of matrix toughness to interlaminar fracture toughness , In: *Application of Fracture Mechanics to Composite Materials*, Friedrich K., Ed., Amsterdam: Elsevier, 159-186 (1989).
36. Bascom et al. Fractrographic analysis of interlaminar fractures , Tough. Comp. *ASTM STP* 937, Johnston N.J. (Ed.), 131-149 (1987).